Electronic Supplementary Material (ESI) for Catalysis Science & Technology

Kinetics of Cyclooctene Hydroformylation for Continuous Homogeneous Catalysis

Sabriye Güven,[a] Bart Hamers,[b] Robert Franke,[b] Markus Priske,[b] Marc Becker[b] and Dieter Vogt*[a,c]

Supporting Information

Semi-batch hydroformylation reactions performed for the kinetic study

SI Table 1 gives the reactions conditions applied in the semi-batch experiments performed to determine the kinetics of cyclooctene hydroformylation.

SI Table 1. Reaction conditions, TOF and rate @ 1st min of rxn, and calculated CO concentration in solution for semi-batch experiments performed in the kinetic study

Entry	T (°C)	$[C.octene]_0$ (M)	P_{CO} (bar)	P_{H2} (bar)	[Rh] x10^4 (M)	Alkene / Rh	TOF @ 1st min (h^{-1})	Rate*100 @ 1st min (M/min)	[CO] (M)
1	60	2.76	20.0	22.5	2.70	10 236	1133	1.41	0.15
2	65	2.55	22.5	22.5	2.25	11 333	1413	1.35	0.18
3	65	2.52	17.5	22.5	2.25	11 200	1227	1.16	0.14
4	65	3.08	17.5	22.5	3.15	9 778	1219	1.96	0.14
5	65	3.04	22.5	22.5	3.15	9 651	1314	2.09	0.18
6	65	2.52	17.5	22.5	3.15	8 000	1257	1.66	0.14
7	65	3.11	22.5	22.5	2.25	13 822	1413	1.64	0.18
8	65	3.08	17.5	22.5	2.25	13 689	1280	1.47	0.14
9	65	2.49	22.5	22.5	3.15	7 905	1333	1.74	0.18
10	70	2.83	20.0	22.5	2.70	10 481	1600	2.03	0.16
11	70	2.80	20.0	22.5	2.70	10 370	1600	2.01	0.16
12	70	2.21	20.0	22.5	2.70	8 185	1422	1.41	0.16
13	70	3.32	20.0	22.5	2.70	12 296	1622	2.41	0.16
14	70	2.52	15.0	22.5	2.70	9 333	1733	1.96	0.12
15	70	2.80	23.8	23.8	2.70	10 370	1578	1.98	0.19
16	70	2.83	21.3	21.3	1.80	15 722	1800	1.52	0.17
17	70	2.80	20.0	22.5	3.60	7 778	1550	2.59	0.16
18	70	2.80	20.0	22.5	2.70	10 370	1533	1.93	0.16
19	70	2.80	20.0	22.5	2.70	10 370	1178	1.48	0.16
20	70	2.80	20.0	22.5	2.70	10 370	1578	1.98	0.16
21	70	2.76	20.0	22.5	2.70	10 222	1622	2.01	0.16
22	75	3.08	17.5	22.5	2.25	13 689	1947	2.24	0.14
23	75	3.08	22.5	22.5	3.15	9 778	1924	3.10	0.18
24	75	2.49	17.5	22.5	3.15	7 905	1981	2.58	0.14
25	75	2.55	22.5	22.5	3.15	8 095	1829	2.44	0.18
26	75	2.52	22.5	22.5	2.25	11 200	1973	1.86	0.18
27	75	2.49	17.5	22.5	2.25	11 067	1733	1.61	0.14
28	75	3.11	22.5	22.5	2.25	13 822	1973	2.29	0.18
29	75	3.11	17.5	22.5	3.15	9 873	2000	3.25	0.14
30	80	2.76	20.0	22.5	2.70	10 222	2422	2.99	0.17

Jet-loop reactor with integrated membrane separation

The basic jet-loop reactor design used in this project has been adopted from earlier work reported in the literature.[1] A drawing of the reactor is given below in SI Figure 1 together with a detailed drawing of the jet nozzle.
For gas-liquid mixtures it is advantageous to apply a downward flow in order to increase the residence time of the gaseous phase.[2] A draft tube is added to the reactor to direct the flow through the nozzle along the body of the reactor, so entrained gas bubbles are pushed down against their buoyancy together with the liquid. An impact plate is placed in a way to allow an opening after the draft tube, and the flow is thus directed back up again, where it is sucked back into the jet enabling a very thorough mixing within the reactor.[3,4] The gas is sucked into the nozzle through an inner tube and the liquid flow goes through the opening between this inner tube and an exchangeable nozzle head, via which the restriction applied to the liquid flow can be adjusted.

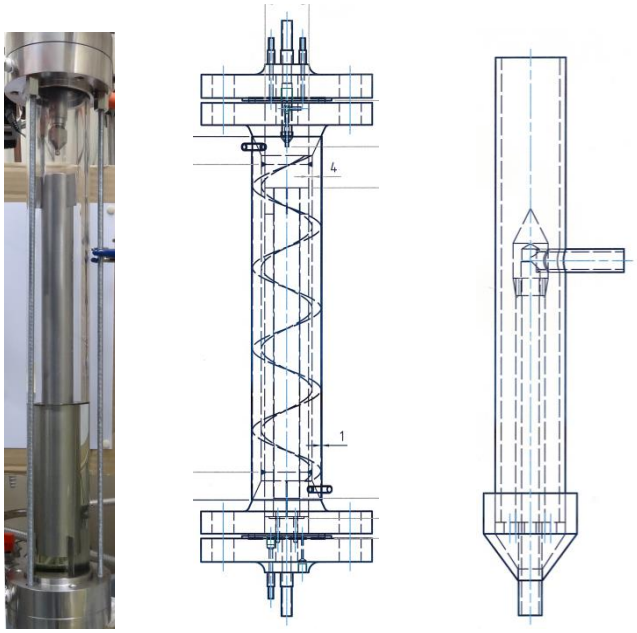

SI Figure 1 Jet-loop reactor (photo of the 1:1 model (left) and drawing (middle)) and the nozzle (right) used in this study

Dimensions belonging to the reactor and the nozzle are given in SI Table 2.

SI Table 2 Dimensions of the jet-loop reactor and the nozzle

D_R: Reactor diameter (cm)	5
L_R: Reactor length (cm)	52
D_D: Draft tube diameters (cm)	1; 2.8
L_D: Draft tube length (cm)	35.5
D_I: Impact plate diameter (cm)	4
L_{DI}: Distance from the lower end of draft tube to impact plate (cm)	2.3
DI_N: Nozzle inner tube inner diameter (mm)	3
DO_N: Nozzle inner tube outer diameter (mm)	4
DI_{NH}: Nozzle restriction head inner diameters (mm)	4.3;4.4;4.6
L_{ND}: Distance from the tip of the nozzle to draft tube (cm)	4.7

There are two different draft tube sizes and the distance between the nozzle head and the upper end of the draft tube, L_{ND}, can be adjusted by lifting the draft tube up on a slide way to the point that the nozzle tip is immersed. There are also 3 different nozzle head diameters to increase/decrease the restriction of the liquid flow at the nozzle.
A list of equipment used in the setup is given in SI Table 3, showing the suppliers and operating window of the equipment and maximum temperature and pressure values where valid.

SI Table 3 List of Equipment used in the reaction setup, their providers and operating range

Equipment	Provider and operation range	P_{max} ,T_{max}
HPLC Pump	Knauer Smarline Pump 100 (0-50 ml/min)	400 bar
Membrane Loop Pump	K-Engineering HMH 060 (20-600 L water/h, gas content max 30%)	100 bar, 200°C
Reaction Loop Pump	K-Engineering HMH 070 (20-900 L water/h, gas content max 30%)	100 bar, 200°C
Level Sensor	Honsberg Nivolock NL-015HS/HK	160 bar, 100°C
Sampling valve	Rhodeyne MX Series II MXP7900-000	414 bar, 50°C
Flow meters	KEM-Küppers Electromechanik HM 005 R05.G.TC.15 (0.8 to 6 L/min)	630bar, 150C
Mass Flow Controller	Bronkhorst HI-TECH Model F-231M-TAD-33-V Multi-Bus DMFC (0-500 ml/min)	
Membrane	Inopor TiO_2, 450 D, 0.9nm pore size, 0.011 m^2 filtration area, channel diameter 7 mm, external 10 mm, length 0.5 m	

The reactor also has a high pressure window, equipped with a live web-cam, which allows to observe the reactor behaviour under reaction conditions at all times. SI Figure 2 shows pictures taken with this camera.

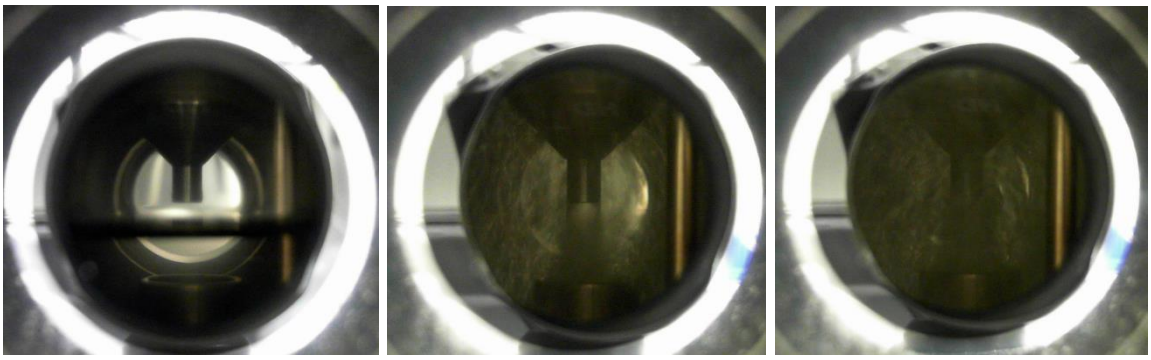

SI Figure 2 Pictures taken through the high pressure window: Liquid at the designated level (left), reaction loop pump running at 1.2 L/min (middle) and pump running at 2.1 L/min (right)

Prediction of cyclooctene concentration over time for continuous reaction

Time dependent concentration data for the estimated reaction profile was obtained by integrating the CSTR design equation given below in Equation 1 with the initial condition that concentration in the reactor at time=0 is Ccyclooctene,0 and replacing cyclooctene with the rate equation given in the manuscript.

$$\frac{dC_{cyclooctene}}{dt} = \frac{1}{\tau}\left(C_{cyclooctene,f} - C_{cyclooctene}\right) - r_{cyclooctene} \quad (1)$$

Concentration as a function of time can then be expressed as given in Equation 2 below:

$$C_{cyclooctene}(t) = C_{cyclooctene,0}\exp\left(-\left(\frac{1}{\tau}+\epsilon\right)t\right) + \frac{C_{cyclooctene,f}}{1+k\tau}\left(1-\exp\left(-\left(\frac{1}{\tau}+\epsilon\right)t\right)\right) \quad (2)$$

where

$$\epsilon = \frac{Aexp(\frac{-E_A}{RT})[Rh]}{1+[CO]/\mathrm{K}} \quad (3)$$

calculated for given conditions using the parameter estimates reported in the manuscript.

Determination of volumetric mass transfer coefficient $k_l a$

We performed $k_l a$ measurements with toluene and a real reaction mixture of 1-pentene hydroformylation ([1-pentene]= 0.493 M, [2-pentene]= 0.073 M, [branched aldehydes]= 0.012 M, [hexanal]= 0.031 M, [toluene]= 2.575 M, [decane]= 0.003 M) in the jet loop reactor, using the batch absorption method. The experimental procedure was adopted from literature for these measurements with slight alterations.[5]Using the mole balance for gas dissolved in the liquid, given in Equation 1, it is possible to obtain Equation 4 below using ideal gas law and Henry's law, detailed derivation of which is reported.[5]

$$\frac{P_2 - P_0}{P_1 - P_0} ln\left(\frac{P_1 - P_2}{P - P_2}\right) = k_l a.\, t \qquad (4)$$

Using this equation, it is possible to deduce $k_l a$ as slope of the line plotted for the left part of Equation 4 vs time. P_0 in the equation is the equilibrium pressure in the reactor before pressure is increased very quickly to P_1 and the mixing is started immediately; in our case by starting the reaction and membrane loop pumps. P_2 is the equilibrium pressure reached as the liquid is saturated with gas again. Pressure values over time are recorded from the start of mixing to the point at which a new equilibrium is reached to plot the mentioned graph. SI Figure 3 below shows the graphs plotted to determine the volumetric syngas transfer rate to toluene at 40°C at different specific power input values.

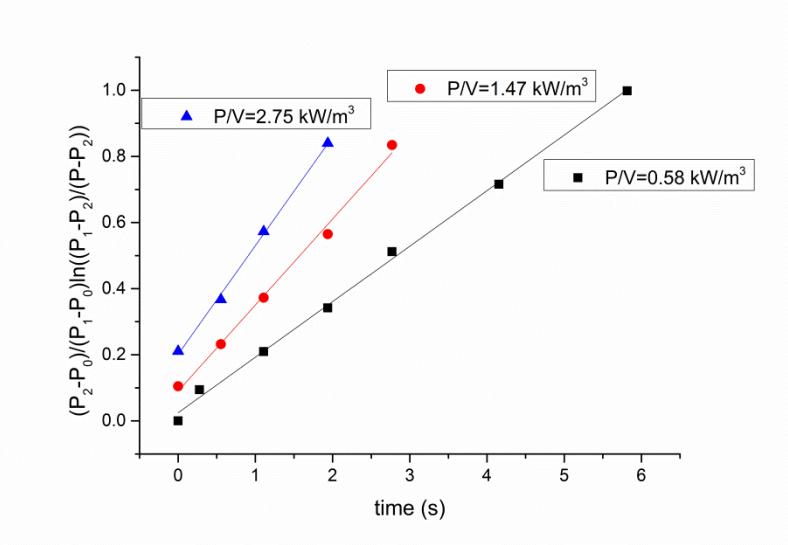

SI Figure 3 Determination of syngas-toluene gas-liquid mass transfer coefficient kla for the jet-loop reactor, performed at different specific power input values

We performed batch absorption experiments at 3 different temperatures for toluene, and also at different P/V values. Furthermore, we determined the $k_l a$ values for the 1-pentene hydroformylation reaction mixture also for a range of specific power input values. Figure 4 below shows the $k_l a$ values obtained as a function of P/V.

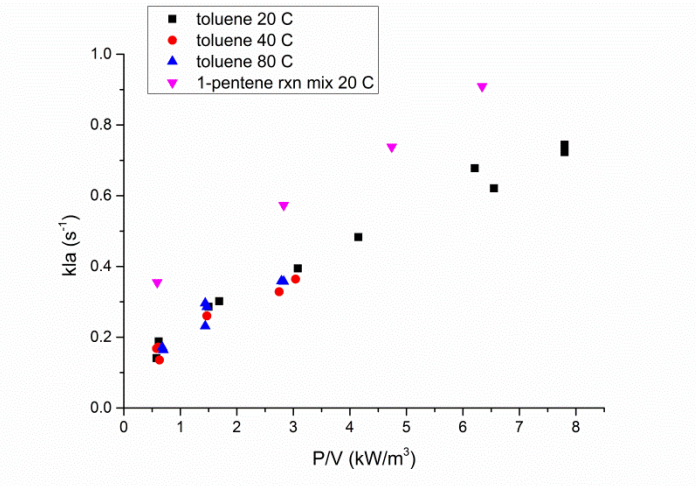

SI Figure 4 Syngas-toluene/1-pentene rxn mixture ([1-pentene]= 0.493 M, [2-pentene]= 0.073 M, [branched aldehydes]= 0.012 M, [hexanal]= 0.031 M, [toluene]= 2.575 M, [decane]= 0.003 M) gas-liquid volumetric mass transfer coefficient $k_l a$ for the jet-loop reactor, performed at different specific power input values and temperatures

As seen in SI Figure 4, $k_l a$ for toluene is not temperature dependent in the temperature range we investigated and increases with increasing specific power input. It is possible to fit a curve to describe the P/V dependence of $k_l a$ as given in Equation 5 for the toluene data at 20°C, with $R^2 = 0.985$ and it can be used to predict the $k_l a$ value for syngas-toluene at least till up to 80°C as well.

$$k_l a\ (toluene\ 20\ ℃) = 0.2188\left(\frac{P}{V_R}\right)^{0.5813} \quad (5)$$

The $k_l a$ values found for the reaction mixture of 1-pentene are higher than those found for toluene, as expected, according to the previous discussion on the improvement of bubble sizes in the presence of polar aldehydes. Equation 8 describes $k_l a$ as a function of P/V for the reaction mixture, with $R^2 = 0.972$.

$$k_l a\ (1-pentene\ rxn\ mix\ 20\ ℃) = 0.4199\left(\frac{P}{V_R}\right)^{0.3776} \quad (6)$$

According to these results, we do not expect $k_l a$ values smaller than 0.1 s^{-1} in the jet-loop reactor during hydroformylation.

1. M. Becker, Technische Universität Dortmund, 2010.
2. M. Velan and T. K. Ramanujam, *Can. J. Chem. Eng.*, 1991, **69**, 1257–1261.
3. A. Behr, M. Becker, and J. Dostal, *Chem. Eng. Sci.*, 2009, **64**, 2934–2940.
4. P. Zehner, A. Ulonska, and R. Paciello, 2003, US 6642420.
5. A. Deimling, B. M. Karandikar, Y. T. Shah, and N. L. Carr, *Chem. Eng. J.*, 1984, **29**, 127–140.